JCB

Tsoumpekos et al., https://doi.org/10.1083/jcb.201705104

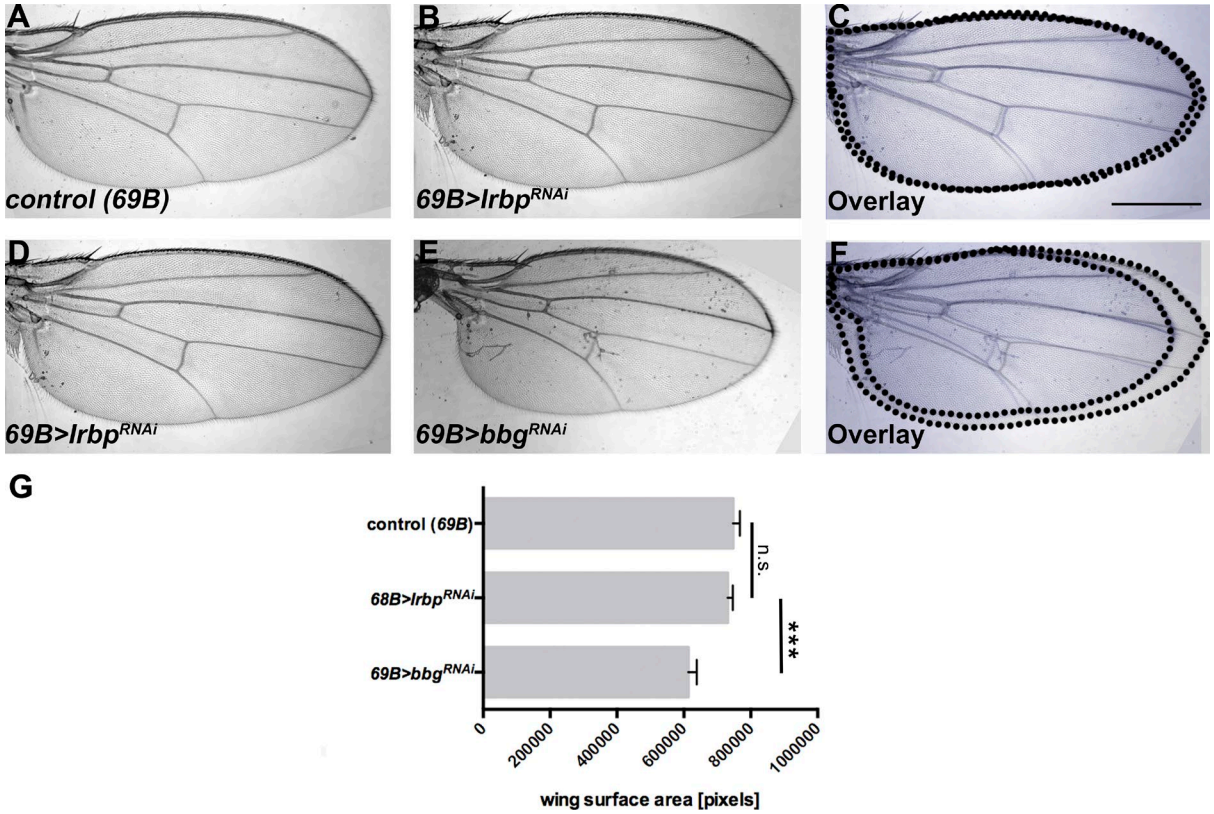

Figure S1. **Reduction of *Irbp* does not affect wing growth. (A–C)** Control (*69B-Gal4*) wing (A), wing expressing *UAS-Irbp*^{RNAi} with *69B-Gal4* (B), and overlay (C). **(D–F)** Wing expressing *UAS-Irbp*^{RNAi} with *69B-Gal4* (D), wing expressing *UAS-bbg*^{RNAi} with *69B-Gal4* (E), and overlay (F). **(G)** Measurement of the wing surface area of 15 independent females per genotype. The statistical analysis (G) used *t* test and ANOVA. ***, $P \leq 0.001$. Error bars show SD. Bar, 500 µm.

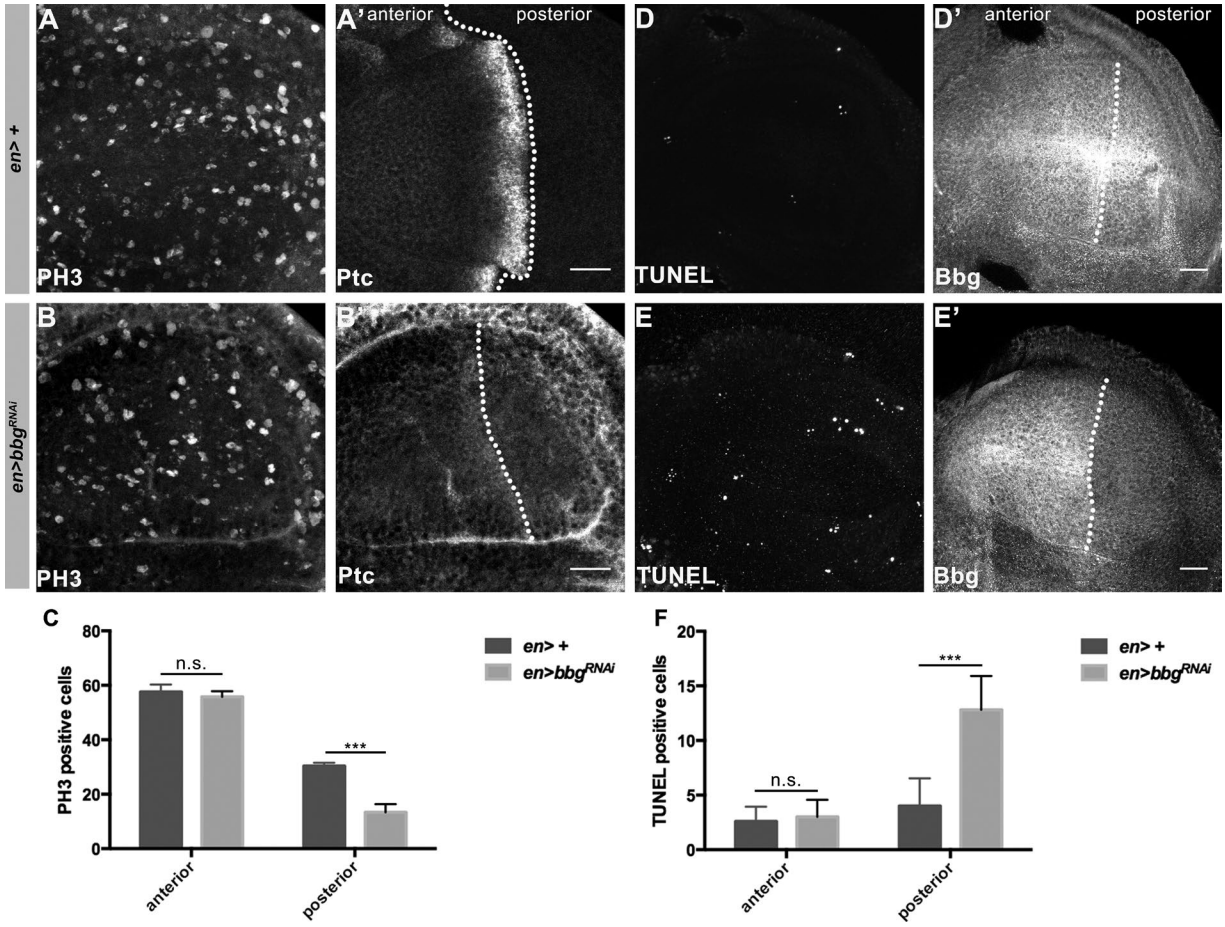

Figure S2. **RNAi-mediated reduction of *bbg* results in reduced cell numbers and increased apoptosis in L3 wing discs.** *en*-Gal4 and *en-Gal4; UAS-bbg^{RNAi}* L3 wing discs stained with anti-PH3/anti-Ptc (A–B′) and TUNEL/anti-Bbg (C–D′), respectively. The dotted lines highlight the AP boundary. **(C and F)** Quantification of PH3-positive cells (C) and TUNEL positive cells (F) in the anterior (control) and posterior (reduced *bbg*) compartment, based on eight independent L3 wing discs per genotype. The statistical analysis (C and F) used *t* test and ANOVA. ***, $P \leq 0.01$; ***, $P \leq 0.001$. Error bars show SD. Bars, 25 µm. Ptc, Patched.

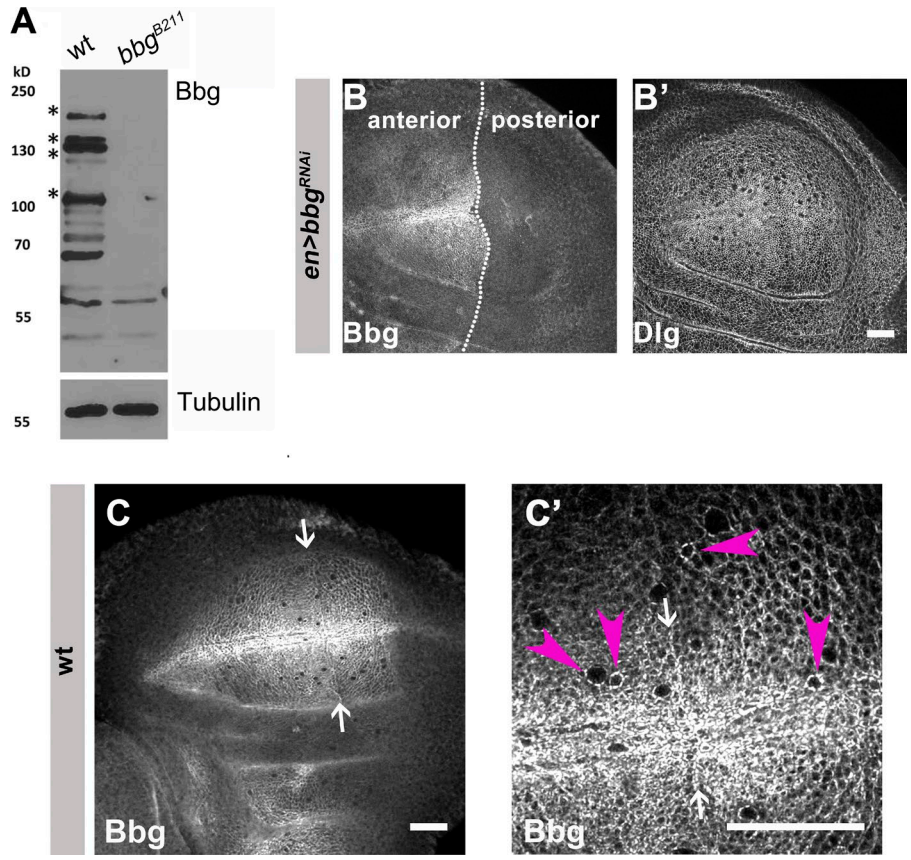

Figure S3. **The anti-Bbg antibody specifically detects Bbg molecules. (A)** WB of lysates prepared from adult abdomen of WT and *bbg*^{B211} female flies. The asterisks point to the predicted isoforms of Bbg. **(B and B′)** Expression of UAS-*bbg*^{RNAi} with *en-Gal4* in the posterior compartment of L3 wing disc abolishes Bbg protein, but leaves Dlg unaffected. The dotted line in B highlights the AP boundary. **(C and C′)** WT L3 wing disc stained with anti-Bbg. (C′) Magnification of the central pouch area of the L3 wing disc shown in C. White arrows in C and C′ mark the AP boundary. Magenta arrowheads in C′ show the enrichment of Bbg in the cytocortex of dividing cells. Bars, 25 µm.